https://doi.org/10.5194/cp-2020-84
Preprint. Discussion started: 26 June 2020

Climate of the Past Discussions

Cold season warming in the North Atlantic during the last 2,000 years: Evidence from Southwest Iceland

Nora Richter[1, 2], James M. Russell[1], Johanna Garfinkel[1], Yongsong Huang[1]

[1] Department of Earth, Environmental and Planetary Sciences, Brown University, Providence, RI 02912, USA
[2] The Josephine Bay Paul Center for Comparative Molecular Biology and Evolution, Marine Biological Laboratory, Woods Hole, MA, 02543, USA

Correspondence to: Nora Richter (nora_richter@brown.edu)

Abstract. Temperature reconstructions from the Northern Hemisphere (NH) generally indicate cooling over the Holocene which is often attributed to decreasing summer insolation. However, climate model simulations predict that rising atmospheric CO_2 concentrations and the collapse of the Laurentian ice sheet caused mean annual warming during this epoch. This contrast could reflect a bias in temperature proxies, and particularly a lack of proxies that record cold (late fall-early spring) season temperatures, or inaccuracies in climate model predictions of NH temperature. We reconstructed winter-spring temperatures during the Common Era (i.e. the last 2,000 years) using alkenones, lipids produced by Isochrysidales haptophyte algae that bloom during spring ice-off, preserved in sediments from Vestra Gíslholtsvatn (VGHV), southwest Iceland. Our record indicates cold-season temperatures warmed during the last 2,000 years, in contrast to NH averages. Sensitivity tests with a lake energy balance model show that this warming is likely driven by increasing winter-spring insolation. We also found distinct seasonal differences in centennial-scale, cold-season temperature variations in VGHV compared to existing records of summer and annual temperatures from Iceland. Sustained or abrupt cooling in VGHV temperatures are associated with the cumulative effects of solar minima and volcanic eruptions, and potentially ocean and sea-ice feedbacks associated with cooling in the broader Arctic. However, multi-decadal to centennial-scale changes in cold season temperatures were strongly modulated by internal climate variability, i.e. the North Atlantic Oscillation, which can result in winter warming in Iceland even after a major negative radiative perturbation.

https://doi.org/10.5194/cp-2020-84
Preprint. Discussion started: 26 June 2020

Climate of the Past Discussions

1 Introduction

Temperatures in the Northern Hemisphere (NH) are generally thought to have cooled over the past 2,000 years, culminating in the Little Ice Age (LIA, c. 1450-1850 CE) (Kaufman et al., 2009; Seppä et al., 2009; PAGES 2K Consortium, 2013, 2019; McKay and Kaufman, 2014). However, the majority of NH temperature reconstructions are based on proxies that respond to climate change during the warm season and may not capture trends in annual or winter and spring temperatures (Liu et al., 2014; PAGES 2K Consortium, 2019). This limits our understanding of major atmospheric phenomena in the NH, such as the North Atlantic Oscillation (NAO) which dominates wintertime variability, as well as changes in ocean circulation and other phenomena driving variability in the extent of Arctic sea ice.

Many oceanic and atmospheric processes that influence surface climate in the Atlantic and the broader NH are centered in the high North Atlantic region, making it an important location to study changes during the cold season (Hurrell, 1995; Yeager and Robson, 2017). Terrestrial paleoclimate records from Iceland, for instance, have the potential to resolve temperature changes during the cold season as this region is sensitive to the NAO and sits near the southern limit of Arctic sea ice (Hurrell, 1995; Hanna et al., 2004, 2006). The high sedimentation rates in Icelandic lakes, along with well-known volcanic eruptions that can be used as age constraints, make this an ideal location and archive to test how winter and spring temperatures evolved over the past 2,000 years (Axford et al., 2007, 2009; Geirsdóttir et al., 2009, 2019; Gathorne-Hardy et al., 2009; Larsen et al., 2011; Langdon et al., 2011; Holmes et al., 2016). However, existing terrestrial records of temperature from Iceland are limited due to their sensitivity to the warm season, low temporal resolution and length, or compounding effects on proxies from human land-use or precipitation over the past 2,000 years.

Here we present a reconstruction of winter-spring temperatures developed using well-dated lake sediments from southwest Iceland to assess seasonal temperature changes in the North Atlantic climate over the past 2,000 years. We take advantage of alkenone-production by Group I Isochrysidales (i.e. haptophyte algae) during the spring season to develop a record of winter-spring temperatures and investigate the forcings responsible for cold-season temperature changes using a lake energy balance model.

2 Methods

2.1 Study site and age model

Vestra Gíslholtsvatn (VGHV) is a small lake (1.57 km^2) located in southwest Iceland (61 m a.s.l., 63° 56’ N, 20° 31’ W; Fig. 1), about 25 km from the coast (Blair et al., 2015). Mean monthly temperatures range from -1.4 °C during the winter months (DJF) to 10.4 °C during the summer months (JJA) (station at Hella, 1958-2005 CE; Icelandic Meteorological Office). Cores

https://doi.org/10.5194/cp-2020-84
Preprint. Discussion started: 26 June 2020

Climate of the Past Discussions
Open Access
EGU

were collected in 2008 using a Bolivia piston coring system (Blair et al., 2015), and were sampled at the National Lacustrine Core Facility (LacCore) at the University of Minnesota.

The VGHV cores were dated using previously identified tephra, including seven historical and four pre-historical tephra beds (Blair et al., 2015 and references therein). The age model was developed using 'classical' age modeling (CLAM) with a smoothed spline fit. The resulting age model has an uncertainty of 5 to 15 yrs from -50 to 1200 yrs BP and 18 to 83 yrs from 1201 to 2000 yrs BP (Fig. 2; Blaauw, 2010).

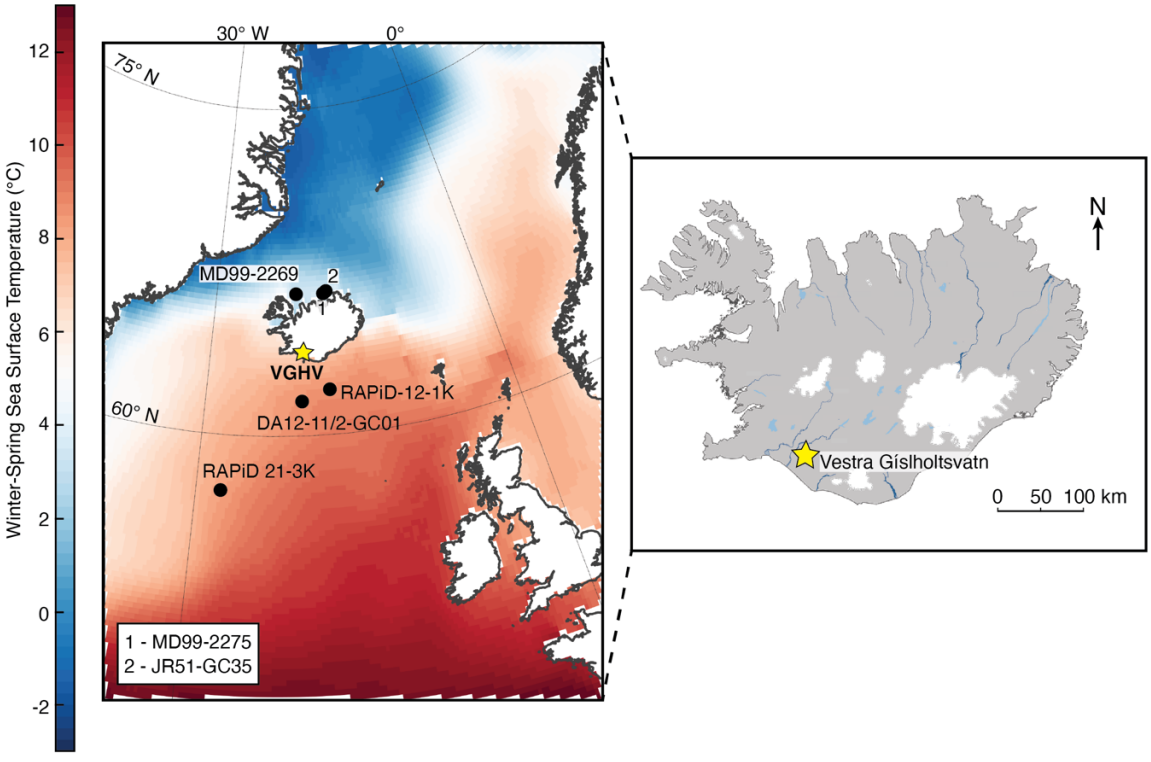

Figure 1. Map of mean winter-spring (DJFMAM) sea surface temperatures from 1955-2017 in the high North Atlantic region. The marine sediment cores MD99-2269 (Moros et al., 2006; Justwan et al., 2008; Cabedo-Sanz et al., 2016), MD99-2275 (Massé et al., 2008; Sicre et al., 2008; Jiang et al., 2015), JR51-GC35 (Cabedo-Sanz et al., 2016), DA12-11/2-GC01 (Van Nieuwenhove et al., 2019), and RAPiD 21-3K (Sicre et al., 2011; Miettinen et al., 2012) that are discussed in the text are indicated. The study site, Vestra Gíslholtsvatn (VGHV), is marked by a yellow star. The maps were made using data from Natural Earth, the National Land Survey of Iceland, and the National Oceanic and Atmospheric Administration (NOAA) World Ocean Database (Boyer et al., 2018).

https://doi.org/10.5194/cp-2020-84
Preprint. Discussion started: 26 June 2020

Climate of the Past Discussions

2.2 Lipid analyses

Sediments were freeze-dried and extracted using a Dionex™ accelerated solvent extraction (ASE 350) system at 120 °C and 1200 psi. All of the extracts were separated by silica gel (40-63 µm, 60 Å) flash chromatography to obtain alkane (hexane; Hex), ketone (dichloromethane; DCM), and polar (methanol; MeOH) fractions. Saponification was used to remove wax esters by dissolving the dried ketone fraction in a 1 molar potassium hydroxide solution with MeOH:H_2O (95:5, v/v) and heating the samples for 3 hrs at 65 °C. 5 % NaCl in H_2O and 50 % HCl in H_2O were added to the samples and the lipid faction was extracted using Hex (100 %). Ketone fractions were further purified using silver nitrate columns (D'Andrea et al., 2007) with DCM (100 %) followed by ethyl acetate (100 %) to elute the alkenones. If additional cleaning was needed, a modified procedure from Salacup et al. (2019) was used. The alkenone fraction was dried under N_2 gas and re-dissolved in 1.5 mL of DCM:Hex (2:1, v/v). To this, a 1.5 mL solution of 100 mg/mL urea in MeOH was added. The resulting crystals were dried under N_2 gas, and the urea addition was repeated two more times. The dried urea crystals were cleaned with Hex (100 %) and extracted as the non-adduct. Milli-Q water was added to the vial to fully dissolve the urea crystals, and the adduct was extracted using Hex (100 %). The samples were then analyzed for alkenones. For several samples, co-eluting compounds were still visible, or concentrations were too low for reliable quantification. These samples were not included in our final reconstruction.

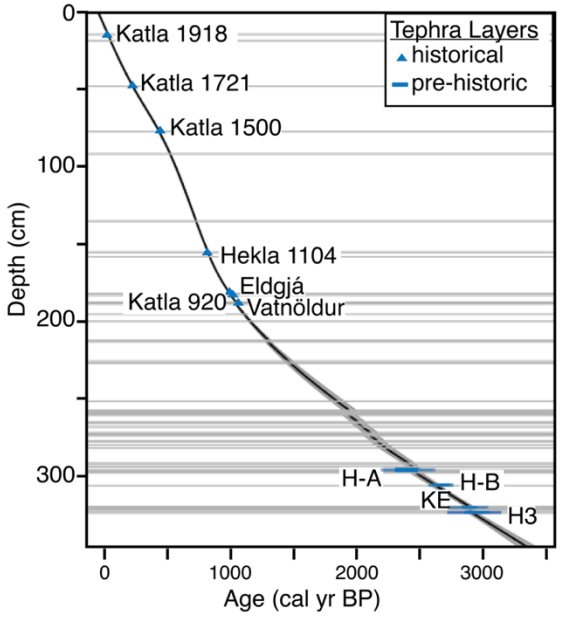

Figure 2. Age model for Vestra Gíslholtsvatn with historic and pre-historic tephra layers (previously identified by Blair et al., 2015 and references therein) used for dating indicated. The gray lines represent tephra layers that were removed from the age model.

https://doi.org/10.5194/cp-2020-84
Preprint. Discussion started: 26 June 2020


Climate of the Past Discussions

The resulting alkenone fraction was analyzed using an Agilent 6890N gas chromatography (GC) and flame ionization detector (FID) system with an Agilent VF-200ms capillary column (60 m x 250 µm x 0.10 µm). Samples were injected into a CIS-PTV inlet in solvent vent mode (6.9 psi at 112 °C). The oven program was set to 50 °C and increased to 235 °C at 20 °C/min and ramped to 320 °C at 1.39 °C/min where it was held isothermally for 5 min. For additional verification or identification of co-eluting compounds, samples were run on an Agilent 6890N GC system coupled with an Agilent 5793 N quadrupole mass spectrometer (MS). All samples were injected with pulsed splitless injection mode (20 psi at 315 °C) and run on an Agilent VF-200ms capillary column (60 m x 250 µm x 0.10 µm). The oven program was started at 40 °C for 1 min, ramped up to 255 °C at 20 °C/min, increased again to 315 °C at 2 °C/min, and then held isothermally for 10 min. The MS ionization energy was set to 70 eV with a scan range of 50 to 600 *m/z*.

2.3 Alkenones as a proxy for lake water temperatures

Alkenones are long-chain ketones produced by Isochrysidales haptophyte algae in both marine and lacustrine environments. Numerous marine-based culture and core-top studies show that variations in alkenone saturation (i.e., changes in $C_{37:3}$Me and $C_{37:2}$Me production) are inversely correlated with temperature, and can be linearly calibrated to temperature using either the U^{K}_{37} or $U^{K'}_{37}$ index (Brassell et al., 1986; Prahl and Wakeham, 1987; Prahl et al., 1988; Müller et al., 1998; Conte et al., 2006). Similarly, culture studies, core tops, and in situ measurements in lakes show that changes in alkenone saturation are also correlated with temperature (Zink et al., 2001; Sun et al., 2007; Toney et al., 2010; D'Andrea et al., 2011, 2012, 2016; Wang and Liu, 2013; Nakamura et al., 2014; Longo et al., 2016, 2018; Zheng et al., 2016). The U^{K}_{37} index can be applied to lacustrine environments and is calculated as follows:

$$U^{K}_{37} = \frac{[C_{37:2}Me] - [C_{37:4}Me]}{[C_{37:2}Me] + [C_{37:3}Me] + [C_{37:3*}Me] + [C_{37:4}Me]} \quad (1)$$

Despite successful application of the U^{K}_{37} index in lakes (D'Andrea et al., 2011, 2012; van der Bilt et al., 2018), regional variability in the relationship between the U^{K}_{37} index and temperature often requires the development of local temperature calibrations (Wang and Liu, 2013; D'Andrea et al., 2016; Longo et al., 2016). Unfortunately, there is currently no local calibration for Icelandic lakes. We further discuss this issue below.

Sedimentary alkenones may derive from multiple alkenone-producing species, mainly Group I and II Isochrysidales, with distinct alkenone signatures and varying responses to temperature (Coolen et al., 2004; Sun et al., 2007; Theroux et al., 2010, 2013; Ono et al., 2012; Toney et al., 2012; Nakamura et al., 2014; D'Andrea et al., 2016). Group I Isochrysidales produces distinct tri-unsaturated alkenones (e.g., $C_{37:3*}$Me), which can be used to test for species-mixing effects with the RIK_{37} index (Longo et al., 2016):

https://doi.org/10.5194/cp-2020-84
Preprint. Discussion started: 26 June 2020


Climate of the Past Discussions

$$RIK_{37} = \frac{[C_{37:3}]}{[C_{37:3} + C_{37:3*}]} \quad (2)$$

A RIK_{37} value of 1.0 suggests a predominance of the $C_{37:3}$Me and the presence of Group II Isochrysidales, while values from 0.48 to 0.63 are empirically shown to correspond to Group I Isochrysidales (Longo et al., 2016, 2018).

2.4 Seasonal temperature sensitivity of Group I alkenones in lakes

In Greenland and Alaska, Group I Isochrysidales bloom during the early spring in the photic zone as lake ice starts to melt (D'Andrea and Huang, 2005; D'Andrea et al., 2011; Longo et al., 2016, 2018). Alkenone production remains high as the lake undergoes isothermal mixing and decreases when thermal stratification begins to develop in late spring/early summer (Longo et al., 2018). This holds true for other Group I-containing lakes in the NH, including lakes in Iceland, as evidenced by the positive correlation between the U^{K}_{37} index and mean spring air temperatures (Longo et al., 2018).

We investigated the controls on spring lake water temperatures and the timing of ice-melt in VGHV using a lake energy balance model (Dee et al., 2018). The model was initialized using ERA-Interim daily data (1979-2019 CE; ECMWF; Dee et al., 2011) averaged over grid cells covering southwest Iceland (18.25° W-22.75° W by 63.00° N-64.50° N for a 0.75° x 0.75° grid). An initial control simulation was run for 30 years, followed by sensitivity tests where various perturbations were introduced.

The perturbation experiments focused on the effects of changes in seasonal air temperatures and shortwave and longwave radiation on lake surface temperatures and ice-off dates. We used instrumental data from Hella, Iceland (1958-2005 CE) to determine the magnitude of seasonal air temperature changes (Icelandic Meteorological Office). In southwest Iceland, the average temperature range for each season is about ± 7 °C, whereas the interannual variability is about ± 3 °C. Based on this we perturbed the ERA interim seasonal air temperature values by -7 °C, -3 °C, 0 °C, +3 °C, and +7 °C and re-ran the lake model with the adjusted parameters. We repeated these experiments, but instead perturbed surface incident shortwave radiation to test how external forcings can drive changes in temperature. Incoming (top of the atmosphere) insolation at 63° N has increased in winter-spring (DJFMAM) by 2.5 W m^{-2} and in spring (MAM) by 3.7 W m^{-2} over the past 2,000 years (Laskar et al., 2004). We therefore tested insolation forcing by perturbing seasonal changes in surface incident shortwave radiation by -4 W m^{-2}, -2 W m^{-2}, 0 W m^{-2}, +2 W m^{-2}, and +4 W m^{-2}. The effects of volcanic eruptions on temperature and ice-off dates were also tested by changing shortwave radiation by -30 W m^{-2}, -10 W m^{-2}, 0 W m^{-2}, +10 W m^{-2}, and +30 W m^{-2}. These values were based on regional radiative feedback studies from the 1783 CE Laki (Oman et al., 2006) and 2010 CE Eyjafjallajökull (Hirtl et al., 2019) eruptions in Iceland. It should be noted that Iceland receives minimal light during the winter months, and values were set to 0 W m^{-2} if a negative perturbation decreased shortwave radiation below 0 W m^{-2}. To

https://doi.org/10.5194/cp-2020-84
Preprint. Discussion started: 26 June 2020

Climate of the Past Discussions
Open Access
EGU

assess the effects of longwave radiation on lake water temperatures and ice-off dates, we decreased and increased incoming longwave radiation by -0.2 W m^{-2}, 0 W m^{-2}, +0.2 W m^{-2}. These values reflect the forcing from well-mixed greenhouse gas (GHG) radiation during the pre-industrial period (Schmidt et al., 2011).

3 Results

3.1 U^K_{37} index: corrections for species-mixing

Our U^K_{37} index from VGHV suggests that there was substantial variability in temperature during the last 2,000 years, but there was also variability in the community of alkenone-producers (Fig. 3a). Alkenones in VGHV surface sediments have a RIK_{37} value of 0.60 and genetic analyses confirm that Group I Isochrysidales is the main alkenone-producer (Longo et al., 2018; Richter et al., 2019). However, the RIK_{37} values increase slightly above the Group I cut-off of 0.63 about c. 500 CE, and then show a more sustained increase after human settlement in Iceland (c. 870 CE), suggesting that Group II alkenone-producers were also present in the lake (Fig. 3b).

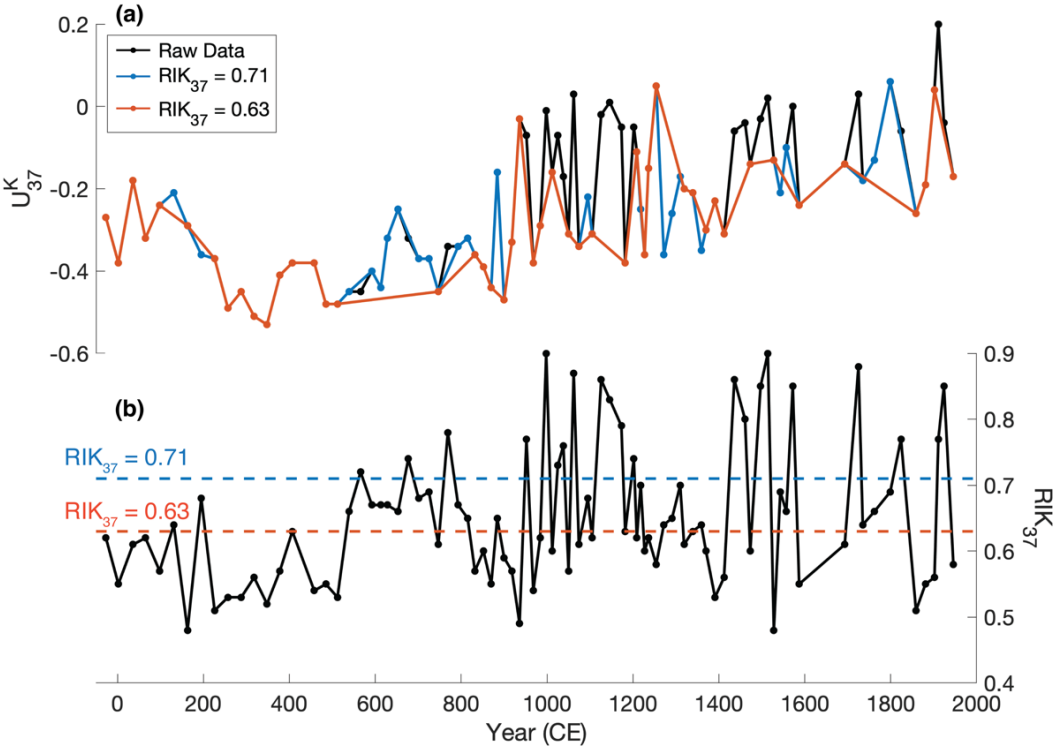

Figure 3. (a) The raw data for the U^K_{37} index is indicated in black, and the corrected U^K_{37} index with a RIK_{37} cut-off of 0.63 and 0.71 are shown in orange and blue, respectively. (b) The original RIK_{37} index is shown below for comparison with the empirical cut-off, RIK_{37} = 0.63, and cut-off for RIK_{37} = 0.71 indicated.

https://doi.org/10.5194/cp-2020-84
Preprint. Discussion started: 26 June 2020

Climate of the Past Discussions

To evaluate the potential impacts of species mixing on the U^K_{37} record, samples with a high abundance of Group II alkenones were removed. We tested several different cut-offs for the RIK_{37} index and compared changes in the mean U^K_{37} values (Fig. 4). If no correction is applied (RIK_{37} = 1.0), then U^K_{37} = -0.34 ± 0.12 from 0-1000 CE and U^K_{37}= -0.14 ± 0.13 from 1001-2000 CE. The empirically defined cut-off of 0.63 yields a mean U^K_{37} index of -0.37 ± 0.12 from 0-1000 CE and -0.20 ± 0.10 from 1001-2000 CE. A less stringent RIK_{37} cut-off at 0.71, results in no significant difference in the mean or the variability of the data (0-1000 CE U^K_{37} = -0.36 ± 0.10 and 1001-2000 CE U^K_{37} = -0.21 ± 0.11). Species mixing thus affects the U^K_{37} temperature record, but regardless of the correction applied to the data, there is an increase in the mean U^K_{37} values (which we interpret as warming) from 0-1000 CE to 1001-2000 CE.

Using a RIK_{37} cut-off of 0.71, the corrected U^K_{37} values and RIK_{37} index are not correlated (r = 0.11, p = 0.35), indicating that species-mixing effects do not affect the final temperature calibration. The resulting U^K_{37} values can be interpreted as a record of temperature changes from Group I alkenones.

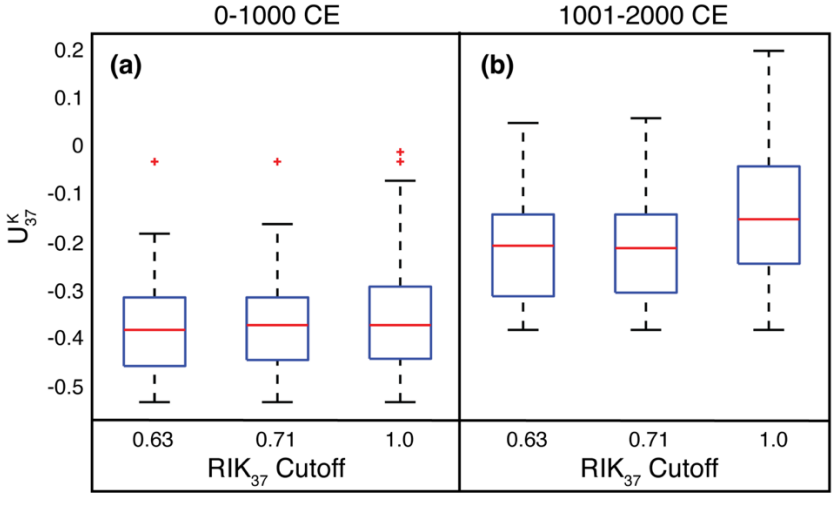

Figure 4. Different RIK_{37} cutoffs applied to the U^K_{37} index for (a) 0-1000 CE and (b) 1001-2000 CE. A RIK_{37} value of 1.0 indicates that the data was not corrected for species-mixing effects, while RIK_{37} = 0.63 corresponds to the empirically defined cut-off for Group I and II (Longo et al., 2018).

3.2 Controls on spring lake water temperature

Results from the lake energy balance model show that seasonal perturbations can have a strong influence on spring lake water temperatures and ice-off dates in VGHV (Fig. 5; Tables S1 and S3). The control run yields an average ice-off date of April 15th with water temperatures on May 1st about 6.6 °C. Air temperature perturbations during the winter (DJF) and spring

https://doi.org/10.5194/cp-2020-84
Preprint. Discussion started: 26 June 2020

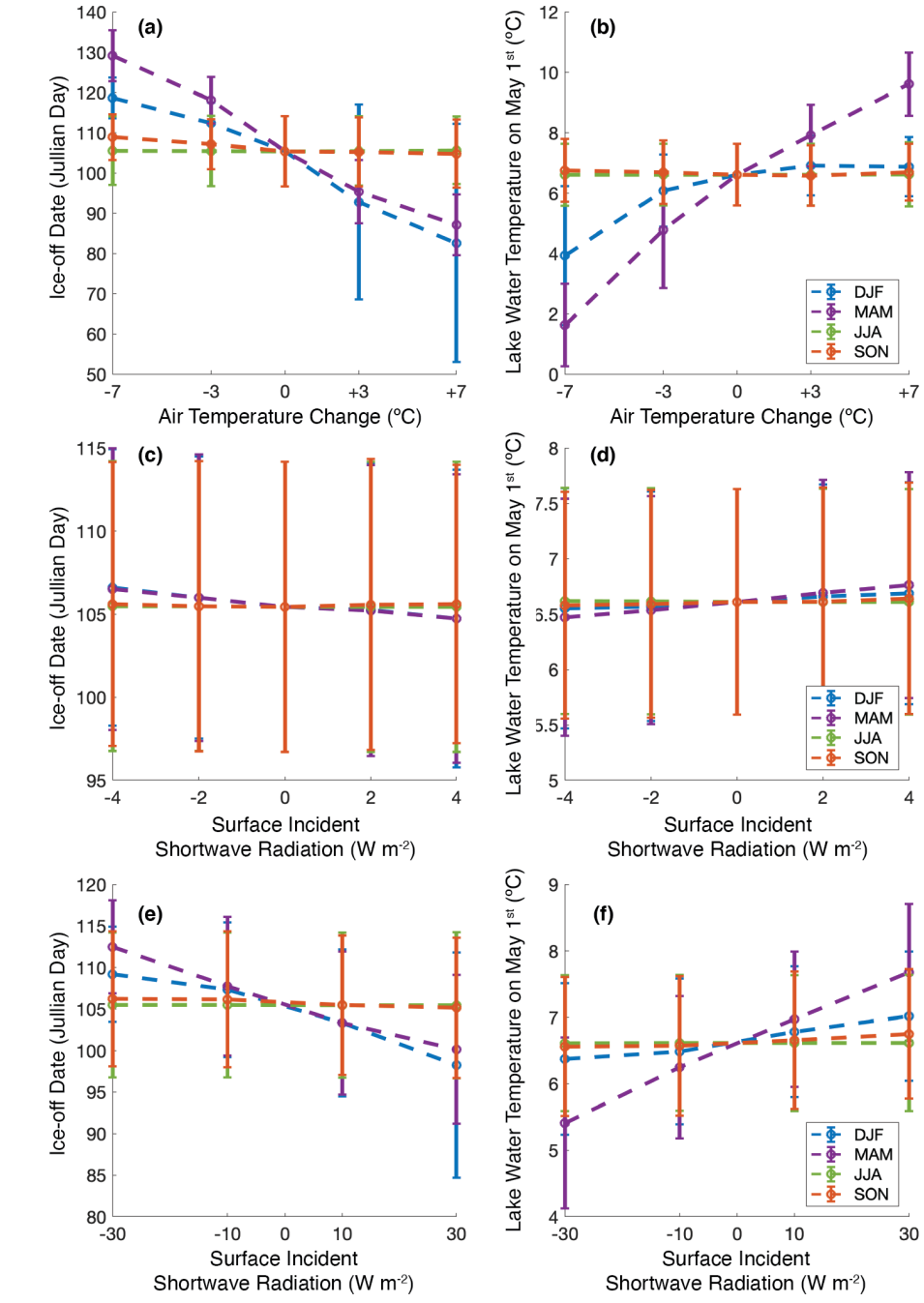

Figure 5. Lake model sensitivity tests showing the impacts of air temperature perturbations during different seasons on (a) ice-off dates and (b) lake water temperatures on May 1st. Similarly, the results for shortwave radiation perturbations that reflect changes in orbital insolation during different seasons for (c) ice-off dates and (d) lake water temperatures and changes from volcanic eruptions for (e) ice-off dates and (f) lake water temperatures are shown. Seasonal changes are shown for winter (DJF, blue), spring (MAM, purple), summer (JJA, green), and fall (SON, orange).

https://doi.org/10.5194/cp-2020-84
Preprint. Discussion started: 26 June 2020


Climate of the Past Discussions

(MAM) alter the timing of ice-off and how rapidly surface water temperatures warm, with warmer air temperatures leading to warmer water temperatures and earlier ice-off dates (Fig. 5a-b). In addition, an increase in shortwave solar radiation during the spring season (MAM) leads to earlier ice-off dates and warmer lake water temperatures (Fig. 5c-d, Table A2). Shorter days during the winter months (DJF) limits the amount of shortwave radiation reaching Iceland, and therefore has a minimal influence on Icelandic temperatures (Fig. 5d and f). Shortwave radiative perturbations from volcanic eruptions during the winter season result in small changes in spring lake water temperatures and ice-off dates, while eruptions during the spring lead to much colder spring water temperatures and later ice-off dates (Fig. 5e-f, Table A2). The increase in longwave radiation from GHGs during the pre-industrial period is relatively small and has no significant influence on either lake water temperatures (change from control = 0.01 ± 1.02 °C) or ice-off dates (change from control = -0.03 ± 8.77 days) (Fig. A1, Table A3). Thus, the timing of the alkenone bloom and the water temperatures recorded by the alkenones are most likely responses to changes in air temperature and temperature changes driven by shortwave solar radiation during the late winter and spring season (DJFMAM).

3.3 Long-term trends and short-term variability in the U^K_{37} record and temperature

The U^K_{37} index can provide temperature estimates using linear relationships that are calibrated in lakes with Group I alkenone-producers (D'Andrea et al. 2011, 2016; Longo et al., 2016, 2018). However, existing lacustrine temperature calibrations provide unreasonable temperature estimates for our site, with large changes in temperature over the past 2,000 years (e.g. calibrations give estimates of 10.2 to 33.5 °C (D'Andrea et al., 2011), 7.1 to 34.4 °C (Longo et al., 2016), 4.4 to 24.5 °C (D'Andrea et al., 2016), -1.4 to 18.3 °C (Longo et al., 2018; see Fig. A2). Given the sensitivity of VGHV lake water temperatures to cold season perturbations and the large variability in winter and spring temperatures observed in instrumental data (mean temperatures in the winter and spring (DJFMAM) season range from -2.4 °C to 3.4 °C with a seasonal variance of 13.1 °C between 1985-2005 at Hella station; Icelandic Meteorological Office), it might be plausible to observe temperature swings close to 10 °C during the spring transitional season (Fig. 5b). Nevertheless, the U^K_{37} index is known to be highly sensitive to temperatures in NH lakes, suggesting that the extreme amplitude of reconstructed temperatures stems from the lack of a local calibration. Therefore, we use the U^K_{37} index to infer and evaluate qualitative changes in temperature trends and variability during the past 2,000 years.

The U^K_{37} record from VGHV, corrected for species mixing, exhibits a long-term trend towards warmer spring lake water temperatures over the past 2,000 years as well as strong multi-decadal to centennial variability (Fig. 6). In particular, a warmer period from the start of our record to c. 200 CE roughly coincides with the Roman Warm Period (RWP) in Northern Europe (Seppä et al., 2009). Cooler temperatures from c. 250-600 CE correspond to the Dark Ages Cold Period (DACP). More variable temperatures, but on average warmer temperatures between c. 850-1100 CE could be associated with the Medieval Climate Anomaly (MCA). The time period usually associated with the LIA is characterized by a warming trend

https://doi.org/10.5194/cp-2020-84
Preprint. Discussion started: 26 June 2020


Climate of the Past Discussions

with an abrupt decrease in the U^{K}_{37} index from c. 1800-1900 CE. However, caution should be used when interpreting results after c. 1400 CE because of low sampling resolution (c. 50 yrs between each sample).

4 Discussion

4.1 Long-term seasonal climate trends in North Atlantic paleoclimate records

In global climate model simulations, rising GHG concentrations and retreating ice sheets during the Holocene lead to warming of global mean annual temperatures, including mean annual temperatures in the NH (Liu et al., 2014). However, temperature reconstructions from the NH typically exhibit a long-term cooling trend during the Holocene (Fig. 6b) (Kaufman et al., 2009; Seppä et al., 2009; PAGES 2K Consortium, 2013, 2019; McKay and Kaufman, 2014). This cooling is often interpreted as a response to decreasing summer insolation. This discrepancy could highlight important deficiencies in climate models and/or feedbacks to NH summer temperatures that influence the temperatures in other seasons or suggest that existing NH temperature reconstructions are biased towards the warm season (Liu et al. 2014). The latter interpretation would imply that insolation has a large influence on seasonal temperatures, with summer cooling and winter warming controlled by increasing and decreasing seasonal insolation, respectively (Fig. 6a). In this case, mean annual temperatures could still be primarily controlled by rising greenhouse gases, particularly at the global scale (Liu et al., 2014).

Winter-spring temperatures from VGHV warm over the past 2,000 years (Fig. 6), and our lake energy balance modeling results show that increasing shortwave radiation and air temperatures during the winter and spring season result in warmer water temperatures and earlier ice-off dates. In contrast, mean annual long-wave radiative forcing, i.e. GHGs, over the pre-industrial period have a minimal influence on water temperatures and ice-off dates. This suggests that the long-term warming trend in VGHV is driven by air temperature changes and solar insolation during the winter and spring season.

Long-term warming trends over the Holocene were also observed in other records of cold-season temperatures in the NH. For instance, pollen records of cold-season temperatures from North America and Europe (Mauri et al., 2015; Marsicek et al., 2018) and an alkenone reconstruction of winter-spring temperatures from Alaska (Longo, 2017) suggest that increasing winter orbital insolation over the Holocene drove warming during the winter season. Winter warming over the Holocene, including the Common Era, was also inferred from chrysophyte cysts in Spain (Pla and Catalan, 2005). An increase in winter sea surface temperatures (SSTs) and a decrease in seasonality over the Holocene is observed in a marine record directly south of Iceland from the North Atlantic subpolar gyre (Van Nieuwenhove et al., 2018). In each of these studies, insolation is proposed as the primary mechanism that is driving changes in seasonal temperatures over the Holocene, supporting the results of our energy balance model.

https://doi.org/10.5194/cp-2020-84
Preprint. Discussion started: 26 June 2020

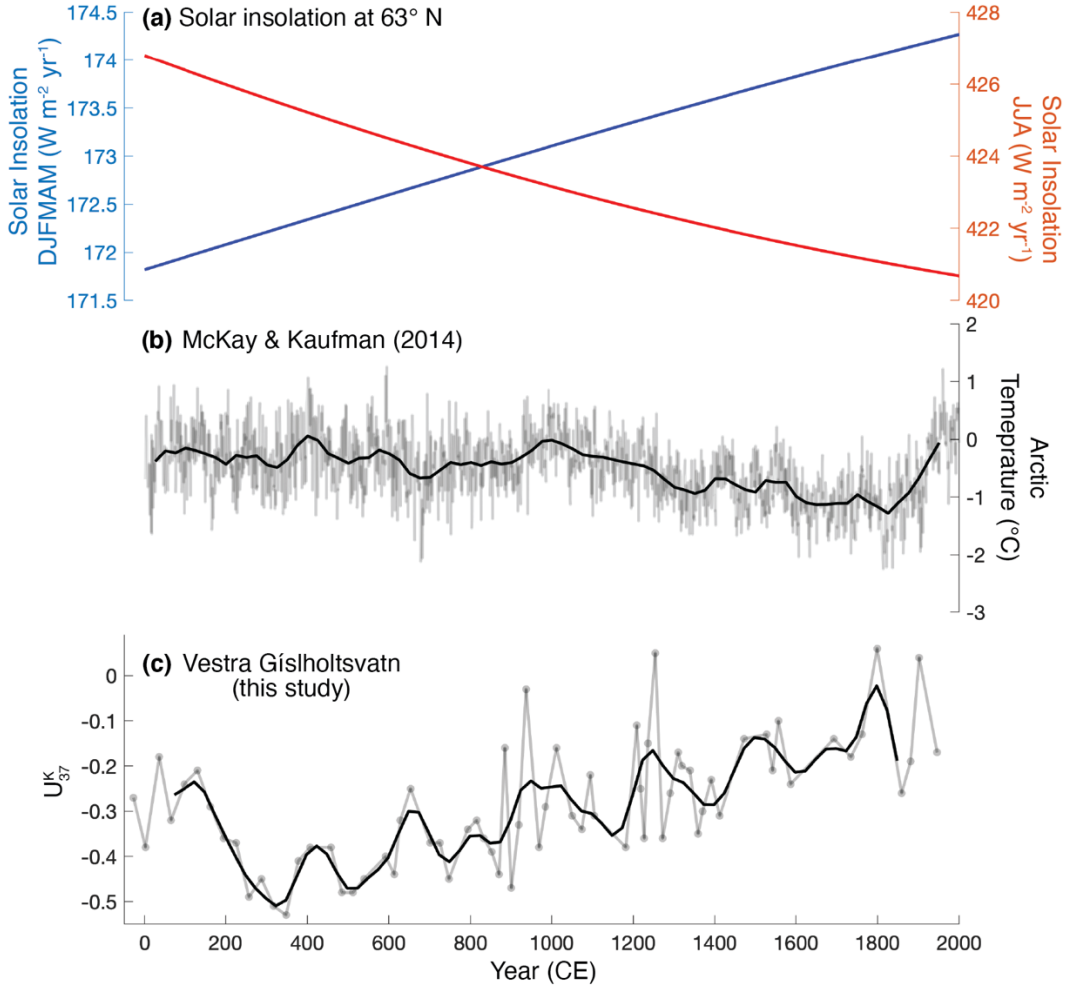

Figure 6. (a) Changes in solar insolation at 63°N for winter-spring (DJFMAM) and summer (JJA) are shown for the past 2,000 years. In addition, (b) a compilation of Arctic temperature reconstructions (McKay and Kaufman, 2014) is shown for comparison with the (e) winter-spring temperature reconstruction from VGHV (the thick black lines for panels (b) and (c) are lowpass filters with data resampled to every 25 years to capture the low-frequency variability of the datasets).

Although there are existing reconstructions of NH cold season temperatures during the Common Era, the high-resolution reconstruction of winter-spring temperatures from VGHV is one of the few sites in the Northern high latitudes where the effects of seasonal insolation on winter temperature can be tested without having to account for the influence of compounding factors on proxy records. For instance, varve thickness records have been interpreted to reflect winter temperatures but might be influenced by human activities in the catchment area, variations in snow accumulation, the timing of spring melt, and changes in precipitation (Ojala and Alenius, 2005; Haltia-Hovi et al., 2007). Varve thickness records from the Arctic that record changes in snow or glacial melt are also used to infer long-term cooling during the melt season;

https://doi.org/10.5194/cp-2020-84
Preprint. Discussion started: 26 June 2020


Climate of the Past Discussions

however, the melt season in the high Arctic often extends well into the summer months (Cook et al., 2009; Larsen et al., 2011) and can be affected by Arctic summer hydrology. Water isotope records from ice cores from Svalbard and a stalagmite from the Central Alps are sensitive to winter air temperatures during the instrumental period, but changes in the moisture source and seasonality of precipitation over time can alter long-term temperature interpretations (Isaksson et al., 2005; Mangini et al., 2005; Divine et al., 2011a, b). In Iceland, records of increasing drift ice along the North Icelandic shelf are sensitive to cold season temperature but are also strongly influenced by different ocean currents and are in direct contrast to records from Western Iceland (Ogilvie et al., 1984; Hopkins, 1991; Moros et al., 2006; Andrews et al., 2019). Although our record lacks a local calibration, we argue that the U^{K}_{37} record from VGHV provides a robust, albeit qualitative, record of cold season temperature given the unique seasonal growth ecology of Group I haptophytes in NH lakes.

The warming trend observed in our new record from Iceland and other records of cold-season temperatures from the NH suggest that long-term temperature changes are driven by a common forcing, mostly orbitally-driven changes in winter and spring insolation (Pla and Catalan, 2005; Mauri et al., 2015; Longo, 2017; Marsicek et al., 2018; Van Nieuwenhove et al., 2018). Our lake model results confirm that water temperatures are sensitive to perturbations in shortwave radiation, indicating that the long-term warming trend observed in the VGHV record is most likely being driven by increasing winter-spring insolation.

4.2 Seasonal multi-decadal to centennial climate variability in the North Atlantic

The VGHV reconstruction of winter-spring temperatures provides an opportunity to test how changes in internal climate variability and external forcings (volcanic eruptions and total solar irradiance, or TSI) influence temperature changes during the cold season in the North Atlantic region. This is important for understanding multi-decadal to centennial climate changes during the cold season and the role of the Atlantic Multi-decadal Variability/Oscillation (AMV/AMO), a low-frequency basin-wide North Atlantic SST anomaly that varies in response to external forcings and internal variability, in driving and/or responding to changes during the cold season (Kerr, 2000; Wang et al., 2017; Yeager and Robson, 2017). The NAO is most active during the winter months, and therefore our record should be particularly sensitive to the NAO and could provide insight into its variability (Hurrell, 1995).

Whether forced or unforced, variability in winter atmospheric circulation, including the NAO, and sea ice extent are often linked to multi-decadal and centennial climate change in the North Atlantic region, particularly over Iceland (e.g. Hanna et al., 2006; Massé et al., 2008; Wang et al., 2017; Yeager and Robson, 2017). In the VGHV record of winter-spring temperatures there is a sharp decrease in the U^{K}_{37} index c. 250 CE and a corresponding increase in drift ice along the North Icelandic shelf (c. 400-900 CE), which coincides with the RWP to DACP transition (Fig. 7; Cabedo-Sanz et al., 2016). Cooling during the DACP is typically attributed to volcanic eruptions and a minimum in solar activity (c. 400-700 CE; Fig. 7a-b); however, the DACP was not uniform across the NH and records differ as to when peak cooling occurred (Steinhilber

https://doi.org/10.5194/cp-2020-84
Preprint. Discussion started: 26 June 2020

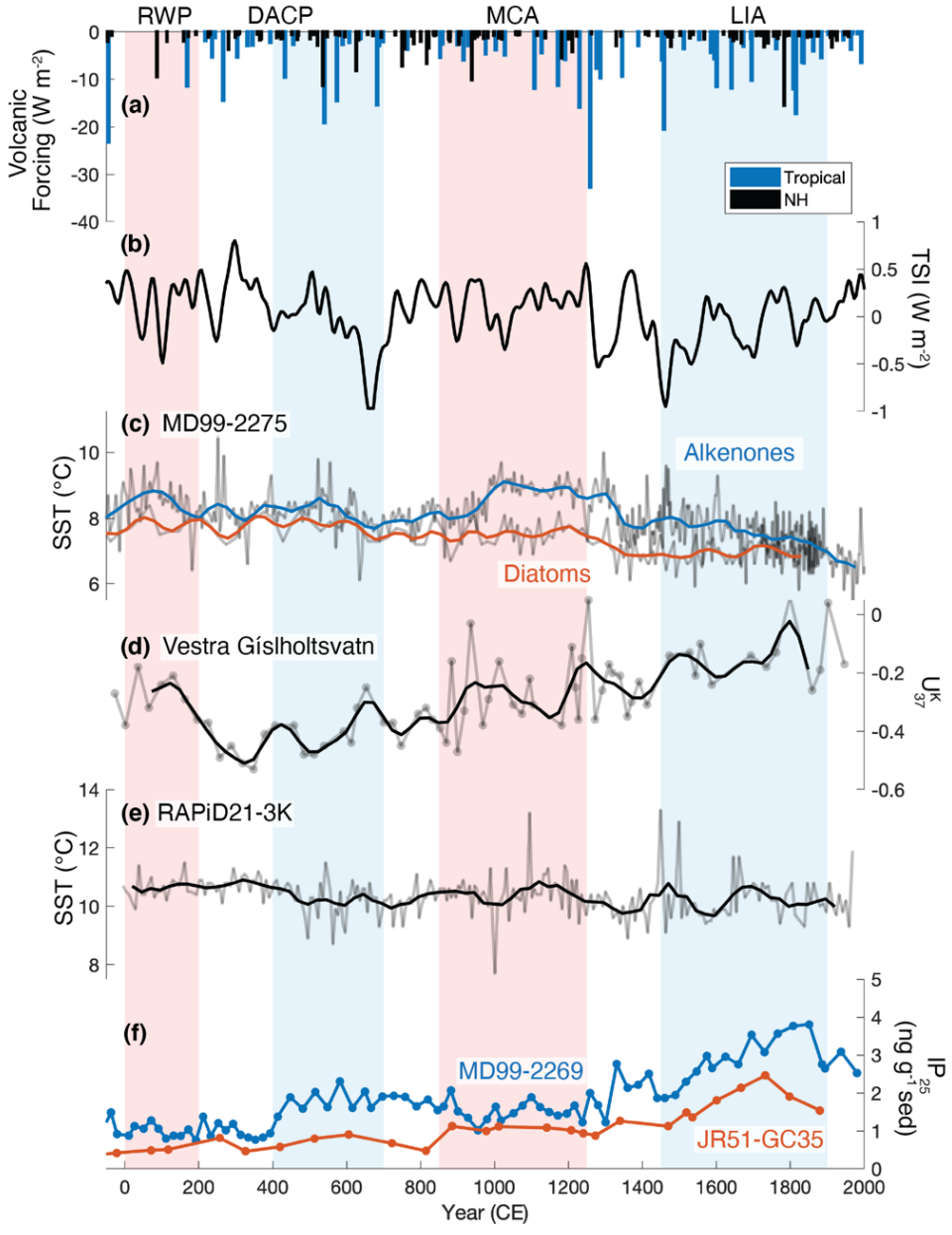

Figure 7. Major changes in radiative forcings over the past 2,000 years, including (a) volcanic forcing from tropical and NH eruptions (Sigl et al., 2015) and (b) changes in total solar irradiance (TSI; Steinhilber et al., 2009) are shown. Marine and terrestrial reconstructions from Iceland are shown, including (c) alkenone and diatom sea surface temperature (SST) reconstructions from core MD99-2275 on the North Icelandic shelf (Sicre et al., 2008; Jiang et al., 2015), (d) an alkenone winter-spring temperature reconstruction from VGHV in southwest Iceland (this study), (e) an alkenone SST record from core RAPiD21-3K in the sub-polar North Atlantic (Sicre et al., 2011), and (f) sea-ice reconstructions developed using IP_{25} from cores MD99-2269 (blue) and JR51-GC35 (orange) from the North Icelandic shelf (Cabedo-Sanz et al., 2016). The timing of major climate anomalies are inferred from Icelandic climate records and include: the Roman Warm Period (RWP, c. 0-200 CE), Dark Ages Cold Period (c. 400-700 CE), Medieval Climate Anomaly (MCA, c. 850-1250 CE), and Little Ice Age (LIA, c. 1450-1900 CE).

https://doi.org/10.5194/cp-2020-84
Preprint. Discussion started: 26 June 2020

et al., 2009; Sigl et al., 2015; Helama et al., 2017). For instance, there is no distinct or prolonged cooling in Iceland SST records during the DACP (Fig. 7c and d), whereas terrestrial records indicate that temperatures were on average cooler between c. 450-700 CE in the Arctic and Northern Europe or c. 500-650 CE in Europe (Sicre et al., 2008, 2011; Kaufman et al., 2009; Miettinen et al., 2012; Jiang et al., 2015; Sigl et al., 2015; Helama et al., 2017). The heterogeneous temperature response is commonly attributed to a prolonged negative phase in the NAO, which would result in more pronounced cooling in Icelandic and Northern European winter temperatures (Helama et al., 2017). Our record would support this interpretation. A negative winter NAO phase does not cause colder NH summer temperatures, which might explain why cooling is not observed in summer temperature reconstructions from tree rings or SSTs before 500 CE (Sicre et al., 2008, 2011; Miettinen et al., 2012; Jiang et al., 2015; Sigl et al., 2015; Helama et al., 2017).

Winter and spring temperatures in VGHV were on average higher between c. 880-1100 CE than temperatures during the DACP but were not stable or particularly warm, unlike the climate usually associated with the Norse settlement of Iceland between c. 870-1100 CE (Fig. 7) (Ogilvie et al., 2000). This time period corresponds to a peak in TSI and weak volcanic activity, which could have triggered a positive phase in the AMV/AMO and warmer summer and annual SSTs near Iceland (Sicre et al., 2008, 2011; Justwan et al., 2008; Ran et al., 2011; PAGES 2K Consortium, 2013; Otto-Bliesner et al., 2016; Wang et al., 2017). Observational data and model results suggest that a positive AMV/AMO can result in more frequent negative NAO phases during the winter, which could explain the cold excursions observed in the VGHV reconstruction and reports of several severe winters in historical records (Ogilvie et al., 1984; Omrani et al., 2014, 2016; Peings and Magnusdottir, 2014).

The 14th-15th centuries mark the start of the LIA and are often associated with a colder-than-average climate in Iceland (Ogilvie et al., 1984; Ogilvie and Jónsson, 2001). In contrast, the VGHV record indicates there was no prolonged cold period during the winter and spring season between c. 1300-1800 CE. Rather, temperatures inferred from the VGHV record varied on multi-decadal to centennial timescales. Cooling during this time period is associated with major volcanic eruptions and decreases in TSI that most likely resulted in a negative AMV/AMO phase and temporary increases in sea ice (Fig. 7; Moros et al., 2006; Massé et al., 2008; Steinhilber et al., 2009; PAGES 2K Consortium, 2013; Cabedo-Sanz et al., 2016; Otto-Bliesener et al., 2016; Wang et al., 2017). In some marine records from Iceland this led to cooling of summer/annual SSTs between c. 1400-1900 CE (Fig. 7c and e; Jiang et al., 2005, 2015; Sicre et al., 2008; Ran et al., 2011).

In the VGHV record, multi-decadal variability and an inconsistent temperature response to major radiative forcings during the LIA suggest that temperature anomalies during the cold season are driven by both forced and unforced variability. For instance, the strong negative radiative forcing after the Samalas eruption (1258 CE) and the Wolf solar minimum (c. 1280-1350 CE) correspond to an increase in drift ice along the North Icelandic shelf and cooling in the VGHV temperature record (Fig. 7; Massé et al., 2008; Steinhilber et al., 2009; Sigl et al., 2015; Cabedo-Sanz et al., 2016). Similarly, the cumulative

https://doi.org/10.5194/cp-2020-84
Preprint. Discussion started: 26 June 2020

effects of the Dalton solar minimum c. 1790-1830 CE and multiple major volcanic eruptions (i.e., Laki 1783 CE, unidentified 1809 CE, and Tambora 1815 CE) in the late 18th and early 19th century could have resulted in enhanced sea ice feedbacks and cooling in VGHV temperatures between c. 1800-1900 CE (Massé et al., 2008; Steinhilber et al., 2009; Zanchettin et al., 2012; Sigl et al., 2015; Cabedo-Sanz et al., 2016; Toohey and Sigl, 2017). Enhanced cooling in the Arctic or colder initial conditions associated with a solar minimum could have dampened the positive NAO response, i.e. winter warming in Iceland and Northern Europe, that is usually observed for two to five winters after volcanic eruptions (Yoshimori et al., 2005; Zanchettin et al., 2012; Ortega et al., 2015; Smith et al., 2016; Sjolte et al., 2018). The inconsistent response in VGHV temperatures to volcanic eruptions and solar minima between c. 1450-1750 CE could be associated with a return to a positive NAO phase that counteracted the effects of negative radiative forcings and led to winter warming over Iceland.

On multi-decadal to centennial timescales, changes in the VGHV record do not consistently correspond to major temperature anomalies observed during the summer months. The differences in seasonal climate responses to external forcings imply that the regional manifestation of these events depends on the initial state of the atmosphere and ocean but is also modulated by internal climate variability (Yoshimori et al., 2005; Zanchettin et al., 2012; Otto-Bliesner et al., 2016; Anchukaitis et al., 2019). For instance, a negative NAO phase coupled with a solar minimum and/or major volcanic eruptions could result in amplified cooling (e.g. Zanchettin et al., 2012; Moffa-Sánchez et al., 2014; Helama et al., 2017; Anchukaitis et al., 2019). Alternatively, the NAO can counteract the effects of major forcings, e.g. a return to a positive NAO phase after a major tropical eruption (Yoshimori et al., 2005; Zanchettin et al., 2012; Ortega et al., 2015; Smith et al., 2016; Sjolte et al., 2018). Discrepancies in regional temperature responses to radiative forcings suggest that unforced variability, namely the NAO, significantly modulates the climate system response on multi-decadal timescales (Yoshimori et al., 2005; Zanchettin et al., 2012; Anchukaitis et al., 2019).

5 Conclusions

The most striking feature of the VGHV record of winter-spring temperatures is a long-term warming trend from c. 250 CE to the present. Gradual warming in cold-season temperatures is most likely driven by increasing winter and spring solar insolation over the last 2,000 years, and contrasts with inferences of mean annual and summer time warming elsewhere in the NH. On multi-decadal timescales winter-spring temperatures are sensitive to strong radiative perturbations, but regional temperature responses can be masked by internal climate variability, namely the NAO. These processes can cause strong contrasts between cold season, warm season, and mean annual temperatures. In general, this highlights a need for more winter and spring temperature reconstructions to improve our understanding of the magnitude and direction of cold-season temperature changes over the Common Era.

https://doi.org/10.5194/cp-2020-84
Preprint. Discussion started: 26 June 2020

Climate of the Past Discussions

Appendix A

Table A1. Lake energy balance model results for air temperature perturbations.

Temperature Perturbation	Ice-off Date (Julian Day)	Water Temperature on May 1st (°C)
Control 0 °C	106 ± 9	6.6 ± 1.0
DJF -7 °C	119 ± 5	3.9 ± 2.3
DJF -3 °C	112 ± 5	6.1 ± 1.2
DJF +3 °C	93 ± 24	6.9 ± 1.0
DJF +7 °C	83 ± 30	6.9 ± 1.0
MAM -7 °C	129 ± 6	1.6 ± 1.4
MAM -3 °C	118 ± 6	4.8 ± 1.9
MAM +3 °C	95 ± 8	7.9 ± 1.0
MAM +7 °C	87 ± 8	9.6 ± 1.0
JJA -7 °C	106 ± 9	6.6 ± 1.0
JJA -3 °C	106 ± 9	6.6 ± 1.0
JJA +3 °C	106 ± 9	6.6 ± 1.0
JJA +7 °C	106 ± 8	6.6 ± 1.0
SON -7 °C	109 ± 6	6.8 ± 1.0
SON -3 °C	107 ± 6	6.7 ± 1.0
SON +3 °C	105 ± 9	6.6 ± 1.0
SON +7 °C	105 ± 9	6.7 ± 1.0

https://doi.org/10.5194/cp-2020-84
Preprint. Discussion started: 26 June 2020


Climate of the Past Discussions

390

Table A2. Lake energy balance model results for shortwave solar radiation perturbations.

Shortwave Solar Radiation Perturbation	Ice-off Date (Julian Day)	Water Temperature on May 1st (°C)
Control	105 ± 9	6.6 ± 1.0
DJF x 0.50	108 ± 8	6.5 ± 1.0
DJF x 0.25	107 ± 8	6.5 ± 1.0
DJF x 1.25	105 ± 9	6.7 ± 1.0
DJF x 1.50	104 ± 9	6.8 ± 1.0
MAM x 0.50	124 ± 8	1.8 ± 1.6
MAM x 0.25	112 ± 9	4.5 ± 1.6
MAM x 1.25	100 ± 8	8.2 ± 1.2
MAM x 1.50	95 ± 7	9.8 ± 1.3
JJA x 0.50	106 ± 9	6.6 ± 1.0
JJA x 0.25	106 ± 9	6.6 ± 1.0
JJA x 1.25	106 ± 9	6.6 ± 1.0
JJA x 1.50	106 ± 8	6.6 ± 1.0
SON x 0.50	106 ± 8	6.5 ± 1.0
SON x 0.25	106 ± 9	6.6 ± 1.0
SON x 1.25	106 ± 8	6.6 ± 1.0
SON x 1.50	105 ± 8	6.7 ± 1.0

Table A3. Lake energy balance model results for longwave radiation perturbations.

Longwave Radiation Perturbation	Ice-off Date (Julian Day)	Water Temperature on May 1st (°C)
Control	105 ± 9	6.6 ± 1.0
-0.2 W m^{-2}	105 ± 9	6.6 ± 1.0
+0.2 W m^{-2}	105 ± 9	6.6 ± 1.0

395

https://doi.org/10.5194/cp-2020-84
Preprint. Discussion started: 26 June 2020

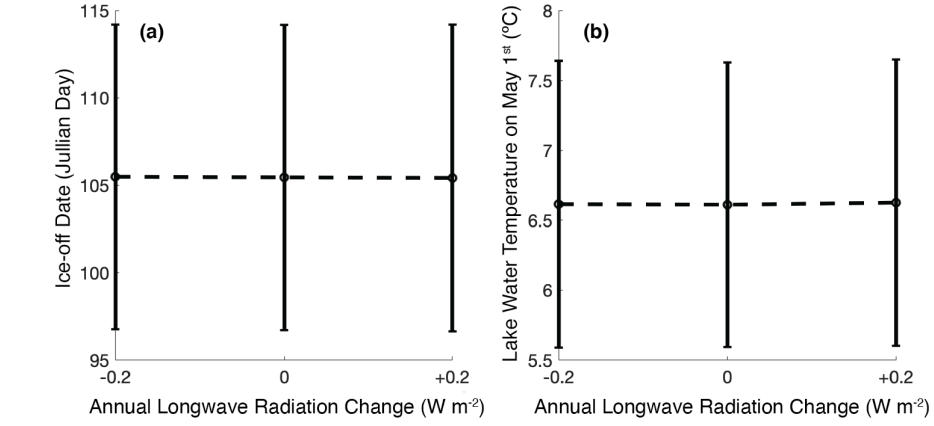

Figure A1. Lake model sensitivity tests showing the effect of annual longwave radiation perturbations on (a) ice-off dates and (b) lake water temperatures on May 1st.

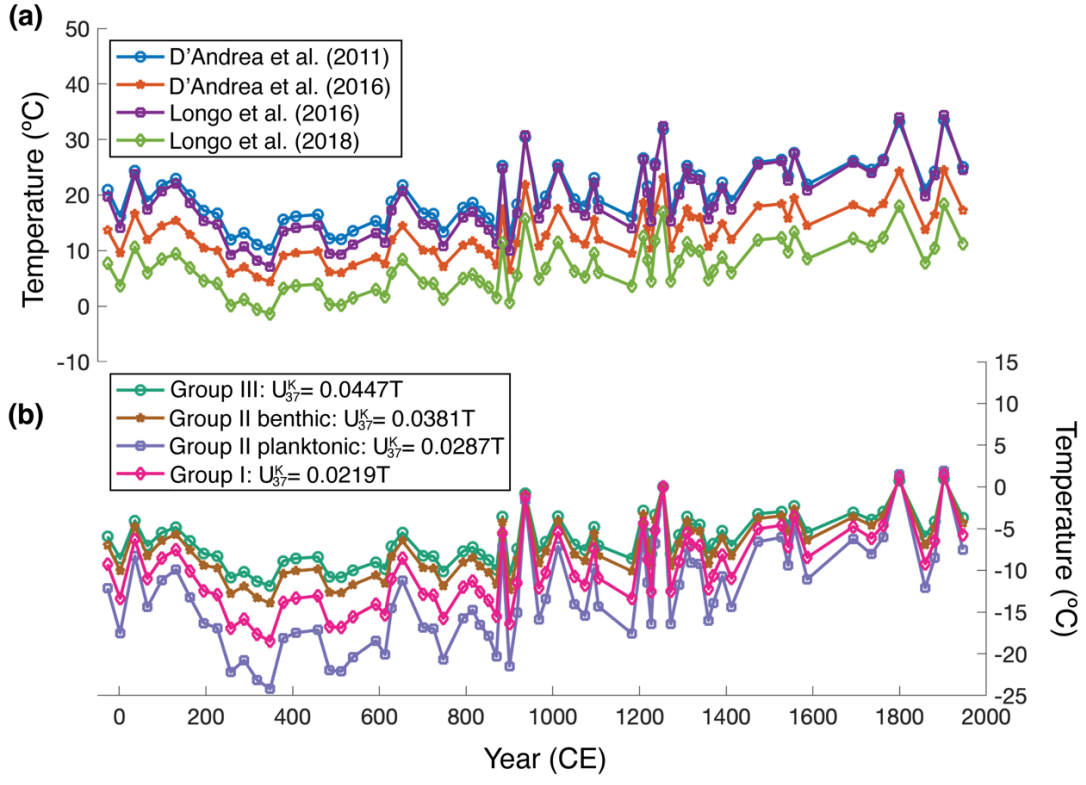

Figure A2. Alkenone calibrations from previous studies including (a) D'Andrea et al., (2011), D'Andrea et al., (2016), Longo et al., (2016), Longo et al., (2018). (b) Different temperatures calculated from slopes previously determined by D'Andrea et al., (2016) for Group III, Group II benthic, Group II planktonic, and Group I.

https://doi.org/10.5194/cp-2020-84
Preprint. Discussion started: 26 June 2020

Data availability

Data will be made available at the National Oceanic and Atmospheric Administration National Centers for Environmental Information (NOAA NCEI) Paleoclimate Database: https://www.ncdc.noaa.gov/paleo/study/29992. The age model and information about the lake sediment core were obtained from Blair et al. (2015). Information about the lake energy balance model used in this study can be found in Dee et al. (2018) and the code for the lake energy balance model is available at: https://github.com/sylvia-dee/PRYSM. ERA-Interim daily data (1979-2019 CE) was obtained from: https://www.ecmwf.int/en/forecasts/datasets/reanalysis-datasets/era-interim (ECMWF; Dee et al., 2011). Meteorological data for southwest Iceland was obtained from: (https://en.vedur.is/climatology/data/; Icelandic Meteorological Office). Data used to make the maps in Fig. 1 can be found at: Natural Earth (https://www.naturalearthdata.com/), the National Land Survey of Iceland (https://www.lmi.is/en/), and the National Oceanic and Atmospheric Administration (NOAA) World Ocean Database (https://www.nodc.noaa.gov/OC5/WOD/pr_wod.html; Boyer et al., in preparation).

Author contributions

Study conceptualized by NR, JMR, and YH. Method development and laboratory analyses by NR and JG. NR prepared the manuscript with contributions from all co-authors.

Competing interests

The authors declare that they have no conflict of interest.

Acknowledgements

This project was funded by Geological Society of America Graduate Student Research Grants, the Nicole Rosenthal Hartnett Graduate Fellowship, Brown University Graduate School, and Brown University Undergraduate Teaching and Research Awards. We would like to thank Prof. T.D. Herbert, R. Rose, Dr. J. Salacup, Dr. G. Weiss, Dr. C. Morrill, A. Neary, and Prof. S.G. Dee for advice and analytical support. All of the samples for this project were obtained from LacCore (National Lacustrine Core Facility), Department of Earth Sciences, University of Minnesota-Twin Cities.

References

Andrews, J. T., Jónsdóttir, I., and Geirsdóttir, Á.: Tracking Holocene drift-ice limits on the northwest–southwest Iceland shelf: Comparing proxy data with observation and historical evidence, Arct. Antarct. Alp. Res., 51, 96-114, https://doi.org/10.1080/15230430.2019.1592648, 2019.

https://doi.org/10.5194/cp-2020-84
Preprint. Discussion started: 26 June 2020

Anchukaitis, K. J., Cook, E. R., Cook, B. I., Pearl, J., D'Arrigo, R., and Wilson, R.: Coupled Modes of North Atlantic Ocean-Atmosphere Variability and the Onset of the Little Ice Age. Geophys. Res. Lett., 46, 12417-12426, https://doi.org/10.1029/2019GL084350, 2019.

Axford, Y., Miller, G.H., Geirsdóttir, Á., and Langdon, P.G.: Holocene temperature history of northern Iceland inferred from subfossil midges. Quat. Sci. Rev., 26, 3344-3358, https://doi.org/10.1016/j.quascirev.2007.09.003, 2007.

Axford, Y., Geirsdóttir, A., Miller, G.H., and Langdon, P.G.: Climate of the Little Ice Age and the past 2000 years in northeast Iceland inferred from chironomids and other lake sediment proxies. J. Paleolimnol., 41, 7-24, https://doi.org/10.1007/s10933-008-9251-1, 2009.

Blaauw, M.: Methods and code for 'classical' age-modelling of radiocarbon sequences. Quat. Geochronol., 5, 512-518, https://doi.org/10.1016/j.quageo.2010.01.002, 2010.

Blair, C. L., Geirsdóttir, Á., and Miller, G. H.: A high-resolution multi-proxy lake record of Holocene environmental change in southern Iceland. J. Quat. Sci., 30, 281-292, https://doi.org/10.1002/jqs.2780, 2015.

Boyer, T.P., Baranova, O. K., Coleman, C., Garcia, H. E., Grodsky, A., Locarnini, R. A., Mishonov, A. V., O'Brien, T.D., Paver, C.R., Reagan, J.R., Seidov, D., Smolyar, I. V., Weathers, K., and Zweng, M. M.: World Ocean Database 2018, (in preparation).

Brassell, S. C., Eglinton, G., Marlowe, I. T., Pflaumann, U., and Sarnthein, M.: Molecular stratigraphy: a new tool for climatic assessment. Nature, 320, 129, https://doi.org/10.1038/320129a0, 1986.

Cabedo-Sanz, P., Belt, S. T., Jennings, A. E., Andrews, J. T., and Geirsdóttir, Á.: Variability in drift ice export from the Arctic Ocean to the North Icelandic Shelf over the last 8000 years: a multi-proxy evaluation. Quat. Sci. Rev., 146, 99-115, https://doi.org/10.1016/j.quascirev.2016.06.012, 2016.

Conte, M. H., Sicre, M. A., Rühlemann, C., Weber, J. C., Schulte, S., Schulz-Bull, D., and Blanz, T.: Global temperature calibration of the alkenone unsaturation index ($U^{K'}_{37}$) in surface waters and comparison with surface sediments. Geochem. Geophy. Geosy., 7, https://doi.org/10.1029/2005GC001054, 2006.

Coolen, M. J., Muyzer, G., Rijpstra, W. I. C., Schouten, S., Volkman, J. K., and Damsté, J. S. S.: Combined DNA and lipid analyses of sediments reveal changes in Holocene haptophyte and diatom populations in an Antarctic lake. Earth Planet. Sci. Lett., 223, 225-239, https://doi.org/10.1016/j.epsl.2004.04.014, 2004.

Cook, T. L., Bradley, R. S., Stoner, J. S., and Francus, P.: Five thousand years of sediment transfer in a high arctic watershed recorded in annually laminated sediments from Lower Murray Lake, Ellesmere Island, Nunavut, Canada. J. Paleolimnol., 41, 77, https://doi.org/10.1007/s10933-008-9252-0, 2009.

D'Andrea, W. J., and Huang, Y.: Long chain alkenones in Greenland lake sediments: Low δ 13C values and exceptional abundance. Org. Geochem., 36, 1234-1241, https://doi.org/10.1016/j.orggeochem.2005.05.001, 2005.

D'Andrea, W. J., Liu, Z., Alexandre, M. D. R., Wattley, S., Herbert, T. D., and Huang, Y.: An efficient method for isolating individual long-chain alkenones for compound-specific hydrogen isotope analysis. Anal. Chem., 79, 3430-3435, https://doi.org/10.1021/ac062067w, 2007.

https://doi.org/10.5194/cp-2020-84
Preprint. Discussion started: 26 June 2020

D'Andrea, W. J., Huang, Y., Fritz, S. C., and Anderson, N. J.: Abrupt Holocene climate change as an important factor for human migration in West Greenland. Proc. Natl. Acad. Sci., 108, 9765-9769, https://doi.org/10.1073/pnas.1101708108, 2011.

D'Andrea, W. J., Vaillencourt, D. A., Balascio, N. L., Werner, A., Roof, S. R., Retelle, M., and Bradley, R. S.: Mild Little Ice Age and unprecedented recent warmth in an 1800 year lake sediment record from Svalbard. Geology, 40, 1007-1010, https://doi.org/10.1130/G33365.1, 2012.

D'Andrea, W. J., Theroux, S., Bradley, R. S., and Huang, X.: Does phylogeny control U^{K}_{37} -temperature sensitivity? Implications for lacustrine alkenone paleothermometry. Geochim. Cosmochim. Acta, 175, 168-180, https://doi.org/10.1016/j.gca.2015.10.031, 2016.

Dee, D. P., Uppala, S. M., Simmons, A. J., Berrisford, P., Poli, P., Kobayashi, S., Andrae, U., Balmaseda, M. A., Balsamo, G., Bauer, P., Bechtold, P., Beljaars, A. C. M., van de Berg, L., Bidlot, J., Bormann, N., Delsol, C., Dragani, R., Fuentes, M., Geer, A. J., Haimberger, L., Healy, S. B., Hersbach, H., Hólm, E. V., Isaksen, L., Kållberg, P., Köhler, M., Matricardi, M., McNally, A. P., Monge-Sanz, B. M., Morcrette, J. J., Park, B. K., Peubey, C., de Rosnay, P., Tavolato, C., Thépaut, J. N., and Vitart, F.: The ERA-Interim reanalysis: configuration and performance of the data assimilation system, Q. J. Roy. Meteor. Soc., 137, 553–597, https://doi.org/10.1002/qj.828, 2011.

Dee, S. G., Russell, J. M., Morrill, C., Chen, Z., and Neary, A.: PRYSM v2. 0: A Proxy System Model for Lacustrine Archives. Paleoceanogr. Paleocl., 33, 1250-1269, https://doi.org/10.1029/2018PA003413, 2018.

Divine, D., Isaksson, E., Martma, T., Meijer, H.A., Moore, J., Pohjola, V., van de Wal, R.S., and Godtliebsen, F.: Thousand years of winter surface air temperature variations in Svalbard and northern Norway reconstructed from ice-core data. Polar Res., 30, 7379, https://doi.org/10.3402/polar.v30i0.7379, 2011a.

Divine, D.V., Sjolte, J., Isaksson, E., Meijer, H.A.J., Van De Wal, R.S.W., Martma, T., Pohjola, V., Sturm, C., and Godtliebsen, F.: Modelling the regional climate and isotopic composition of Svalbard precipitation using REMOiso: a comparison with available GNIP and ice core data. Hydrol. Process., 25, 3748-3759, https://doi.org/10.1002/hyp.8100, 2011b.

Gathorne-Hardy, F.J., Erlendsson, E., Langdon, P.G., and Edwards, K.J.: Lake sediment evidence for late Holocene climate change and landscape erosion in western Iceland. J. Paleolimnol., 42, 413-426, https://doi.org/10.1007/s10933-008-9285-4, 2009.

Geirsdóttir, Á., Miller, G.H., Thordarson, T., and Ólafsdóttir, K.B.: A 2000 year record of climate variations reconstructed from Haukadalsvatn, West Iceland. J. Paleolimnol., 41, 95-115, https://doi.org/10.1007/s10933-008-9253-z, 2009.

Geirsdóttir, Á., Miller, G.H., Andrews, J.T., Harning, D.J., Anderson, L.S., Florian, C., Larsen, D.J., and Thordarson, T.: The onset of Neoglaciation in Iceland and the 4.2 ka event. Clim. Past, 15, 25-40, https://doi.org/10.5194/cp-15-25-2019, 2019.

Haltia-Hovi, E., Saarinen, T., and Kukkonen, M.: A 2000-year record of solar forcing on varved lake sediment in eastern Finland. Quat. Sci. Rev., 26, 678-689, https://doi.org/10.1016/j.quascirev.2006.11.005, 2007.

https://doi.org/10.5194/cp-2020-84
Preprint. Discussion started: 26 June 2020

Hanna, E., Jónsson, T., and Box, J. E.: An analysis of Icelandic climate since the nineteenth century. Int. J. Climatol.: J. Roy. Meteor. Soc., 24, 1193-1210, https://doi.org/10.1002/joc.1051, 2004.

Hanna, E., Jónsson, T., Ólafsson, J., and Valdimarsson, H.: Icelandic coastal sea surface temperature records constructed: putting the pulse on air–sea–climate interactions in the northern North Atlantic. Part I: comparison with HadISST1 open-ocean surface temperatures and preliminary analysis of long-term patterns and anomalies of SSTs around Iceland. J.Clim., 19, 5652-5666, https://doi.org/10.1175/JCLI3933.1, 2006.

Helama, S., Jones, P. D., and Briffa, K. R.: Dark Ages Cold Period: A literature review and directions for future research. Holocene, 27, 1600-1606, https://doi.org/10.1177/0959683617693898, 2017.

Hirtl, M., Stuefer, M., Arnold, D., Grell, G., Maurer, C., Natali, S., Scherllin-Pirscher, B., and Webley, P.: The effects of simulating volcanic aerosol radiative feedbacks with WRF-Chem during the Eyjafjallajökull eruption, April and May 2010. Atmos. Environ., 198, 194-206, https://doi.org/10.1016/j.atmosenv.2018.10.058, 2019.

Holmes, N., Langdon, P. G., Caseldine, C. J., Wastegård, S., Leng, M. J., Croudace, I. W., and Davies, S. M.: Climatic variability during the last millennium in Western Iceland from lake sediment records. Holocene, 26, 756-771, https://doi.org/10.1177/0959683615618260, 2016.

Hopkins, T. S.: The GIN Sea—A synthesis of its physical oceanography and literature review 1972–1985. Earth-Sci. Rev., 30, 175-318, https://doi.org/10.1016/0012-8252(91)90001-V, 1991.

Hurrell, J.W.: Decadal trends in the North Atlantic Oscillation: regional temperatures and precipitation. Science, 269, 676-679, https://doi.org/10.1126/science.269.5224.676, 1995.

Icelandic Meteorological Office: https://en.vedur.is/climatology/data/, last access: 11 June 2020.

Isaksson, E., Divine, D., Kohler, J., Martma, T., Pohjola, V., Motoyama, H., and Watanabe, O.: Climate oscillations as recorded in Svalbard ice core $\omega^{18}O$ records between ad 1200 and 1997. Geogr. Ann. A., 87, 203-214, https://doi.org/10.1111/j.0435-3676.2005.00253.x, 2005.

Jiang, H., Eiríksson, J., Schulz, M., Knudsen, K.L., and Seidenkrantz, M.S.: Evidence for solar forcing of sea-surface temperature on the North Icelandic Shelf during the late Holocene. Geology, 33, 73-76, https://doi.org/10.1130/G21130.1, 2005.

Jiang, H., Muscheler, R., Björck, S., Seidenkrantz, M.S., Olsen, J., Sha, L., Sjolte, J., Eiríksson, J., Ran, L., Knudsen, K.L., and Knudsen, M.F.: Solar forcing of Holocene summer sea-surface temperatures in the northern North Atlantic. Geology, 43(3), 203-206, https://doi.org/10.1130/G36377.1, 2015.

Justwan, A., Koç, N., and Jennings, A.E.: Evolution of the Irminger and East Icelandic Current systems through the Holocene, revealed by diatom-based sea surface temperature reconstructions. Quat. Sci. Rev., 27, 1571-1582, https://doi.org/10.1016/j.quascirev.2008.05.006, 2008.

Kaufman, D. S., Schneider, D. P., McKay, N. P., Ammann, C. M., Bradley, R. S., Briffa, K. R., Miller, G.H., Otto-Bliesner, B.L., Overpeck, J.T., Vinther, B.M., and Lakes, A.: Recent warming reverses long-term Arctic cooling. Science, 325,

1236-1239, https://doi.org/10.1126/science.1173983, 2009.

Kerr, R. A.: A North Atlantic climate pacemaker for the centuries. Science, 288, 1984-1985, https://doi.org/10.1126/science.288.5473.1984, 2000.

Langdon, P.G., Caseldine, C.J., Croudace, I.W., Jarvis, S., Wastegård, S., and Crowford, T.C.: A chironomid-based reconstruction of summer temperatures in NW Iceland since AD 1650. Quat. Res., 75, 451-460, https://doi.org/10.1016/j.yqres.2010.11.007, 2011.

Larsen, D.J., Miller, G.H., Geirsdóttir, Á., and Thordarson, T.: A 3000-year varved record of glacier activity and climate change from the proglacial lake Hvítárvatn, Iceland. Quat. Sci. Rev., 30, 2715-2731, https://doi.org/10.1016/j.quascirev.2011.05.026, 2011.

Laskar, J., Robutel, P., Joutel, F., Gastineau, M., Correia, A. C. M., and Levrard, B.: A long-term numerical solution for the insolation quantities of the Earth. Astron. Astrophys., 428, 261-285, https://doi.org/10.1051/0004-6361:20041335, 2004.

Liu, Z., Zhu, J., Rosenthal, Y., Zhang, X., Otto-Bliesner, B.L., Timmermann, A., Smith, R.S., Lohmann, G., Zheng, W., and Timm, O.E.: The Holocene temperature conundrum. Proc. Natl. Acad. Sci., 111, E3501-E3505, https://doi.org/10.1073/pnas.1407229111, 2014.

Longo, W. M., Theroux, S., Giblin, A. E., Zheng, Y., Dillon, J. T., and Huang, Y.: Temperature calibration and phylogenetically distinct distributions for freshwater alkenones: evidence from northern Alaskan lakes. Geochim. Cosmochim. Ac., 180, 177-196, https://doi.org/10.1016/j.gca.2016.02.019, 2016.

Longo, W.M.: Temperature and terrestrial carbon cycling in Northeastern Beringia since the Last Glacial Maximum: Insights from novel organic geochemical proxies. Ph.D. thesis, Brown University, U.S.A., 277 pp. 2017.

Longo, W.M., Huang, Y., Yao, Y., Zhao, J., Giblin, A.E., Wang, X., Zech, R., Haberzettl, T., Jardillier, L., Toney, J., and Liu, Z.: Widespread occurrence of distinct alkenones from Group I haptophytes in freshwater lakes: Implications for paleotemperature and paleoenvironmental reconstructions. Earth Planet. Sci. Lett., 492, 239-250, https://doi.org/10.1016/j.epsl.2018.04.002, 2018.

Mangini, A., Spötl, C., and Verdes, P.: Reconstruction of temperature in the Central Alps during the past 2000 yr from a $\delta^{18}O$ stalagmite record. Earth Planet. Sci. Lett., 235, 741-751, https://doi.org/10.1016/j.epsl.2005.05.010, 2005.

Marsicek, J., Shuman, B. N., Bartlein, P. J., Shafer, S. L., and Brewer, S.: Reconciling divergent trends and millennial variations in Holocene temperatures. Nature, 554, 92-96, https://doi.org/10.1038/nature25464, 2018.

Massé, G., Rowland, S. J., Sicre, M. A., Jacob, J., Jansen, E., and Belt, S. T.: Abrupt climate changes for Iceland during the last millennium: evidence from high resolution sea ice reconstructions. Earth Planet. Sci. Lett., 269, 565-569, https://doi.org/10.1016/j.epsl.2008.03.017, 2008.

Mauri, A., Davis, B. A. S., Collins, P. M., and Kaplan, J. O.: The climate of Europe during the Holocene: a gridded pollen-based reconstruction and its multi-proxy evaluation. Quat. Sci. Rev., 112, 109-127, https://doi.org/10.1016/j.quascirev.2015.01.013, 2015.

https://doi.org/10.5194/cp-2020-84
Preprint. Discussion started: 26 June 2020

565 Miettinen, A., Divine, D., Koç, N., Godtliebsen, F., and Hall, I.R.: Multicentennial variability of the sea surface temperature gradient across the subpolar North Atlantic over the last 2.8 kyr. J. Clim. 25, 4205-4219, https://doi.org/10.1175/JCLI-D-11-00581.1, 2012.

Moffa-Sánchez, P., Born, A., Hall, I. R., Thornalley, D. J., and Barker, S.: Solar forcing of North Atlantic surface temperature and salinity over the past millennium. Nat. Geosci., 7, 275-278, https://doi.org/10.1038/ngeo2094, 2014.

570 Moros, M., Andrews, J. T., Eberl, D. D., and Jansen, E.: Holocene history of drift ice in the northern North Atlantic: Evidence for different spatial and temporal modes. Paleoceanography, 21, https://doi.org/10.1029/2005PA001214, 2006.

Müller, P. J., Kirst, G., Ruhland, G., Von Storch, I., and Rosell-Melé, A.: Calibration of the alkenone paleotemperature index $U^{K'}_{37}$ based on core-tops from the eastern South Atlantic and the global ocean (60° N-60° S). Geochim. Cosmochim. Ac., 62, 1757-1772, https://doi.org/10.1029/2005GC001054, 1998.

575 Nakamura, H., Sawada, K., Araie, H., Suzuki, I., and Shiraiwa, Y.: Long chain alkenes, alkenones and alkenoates produced by the haptophyte alga Chrysotila lamellosa CCMP1307 isolated from a salt marsh. Org. Geochem., 66, 90-97, https://doi.org/10.1016/j.orggeochem.2013.11.007, 2014.

National Land Survey of Iceland: https://www.lmi.is/en/, last access: 24 June 2020.

Natural Earth: https://www.naturalearthdata.com/, last access: 24 June 2020.

580 Ogilvie, A. E.: The past climate and sea-ice record from Iceland, Part 1: Data to AD 1780. Clim. Change, 6, 131-152, https://doi.org/10.1007/BF00144609, 1984.

Ogilvie, A. E., Barlow, L. K., and Jennings, A. E.: North Atlantic climate c. AD 1000: Millennial reflections on the Viking discoveries of Iceland, Greenland and North America. Weather, 55, 34-45, https://doi.org/10.1002/j.1477-8696.2000.tb04028.x, 2000.

585 Ogilvie, A. E., and Jónsson, T.: "Little Ice Age" research: A perspective from Iceland. Clim. Change, 48, 9-52, https://doi.org/10.1007/978-94-017-3352-6_1, 2001.

Ojala, A. E., and Alenius, T.: 10,000 years of interannual sedimentation recorded in the Lake Nautajärvi (Finland) clastic–organic varves. Palaeogeogr., Palaeoclimatol., Palaeoecol., 219, 285-302, https://doi.org/10.1016/j.palaeo.2005.01.002, 2005.

590 Oman, L., Robock, A., Stenchikov, G. L., Thordarson, T., Koch, D., Shindell, D. T., and Gao, C.: Modeling the distribution of the volcanic aerosol cloud from the 1783–1784 Laki eruption. J. Geophys. Res.: Atmos., 111, https://doi.org/10.1029/2005JD006899, 2006.

Omrani, N. E., Keenlyside, N. S., Bader, J., and Manzini, E.: Stratosphere key for wintertime atmospheric response to warm Atlantic decadal conditions. Clim. Dyn., 42, 649-663, https://doi.org/10.1007/s00382-013-1860-3, 2014.

595 Omrani, N. E., Bader, J., Keenlyside, N. S., and Manzini, E.: Troposphere–stratosphere response to large-scale North Atlantic Ocean variability in an atmosphere/ocean coupled model. Clim. Dyn., 46, 1397-1415, https://doi.org/10.1007/s00382-015-2654-6, 2016.

https://doi.org/10.5194/cp-2020-84
Preprint. Discussion started: 26 June 2020

Ono, M., Sawada, K., Shiraiwa, Y., and Kubota, M.: Changes in alkenone and alkenoate distributions during acclimatization to salinity change in Isochrysis galbana: Implication for alkenone-based paleosalinity and paleothermometry. Geochem. J., 46, 235-247, https://doi.org/10.2343/geochemj.2.0203, 2012.

Ortega, P., Lehner, F., Swingedouw, D., Masson-Delmotte, V., Raible, C. C., Casado, M., and Yiou, P.: A model-tested North Atlantic Oscillation reconstruction for the past millennium. Nature, 523, 71-74, https://doi.org/10.1038/nature14518, 2015.

Otto-Bliesner, B. L., Brady, E. C., Fasullo, J., Jahn, A., Landrum, L., Stevenson, S., Rosenbloom, N., Mai, A., and Strand, G.: Climate variability and change since 850 CE: An ensemble approach with the Community Earth System Model. B.Am. Meteorol. Soc., 97, 735-754, https://doi.org/10.1175/BAMS-D-14-00233.1, 2016.

PAGES 2K Consortium: Continental-scale temperature variability during the past two millennia. Nat. Geosci., 6, 339-346, https://doi.org/10.1038/ngeo1797, 2013.

PAGES 2K Consortium: Consistent multi-decadal variability in global temperature reconstructions and simulations over the Common Era. Nat. Geosci., 12, 643-649, https://doi.org/10.1038/s41561-019-0400-0, 2019.

Peings, Y., and Magnusdottir, G.: Wintertime atmospheric response to Atlantic multidecadal variability: Effect of stratospheric representation and ocean–atmosphere coupling. Clim. Dyn., 47, 1029-1047, https://doi.org/10.1007/s00382-015-2887-4, 2016.

Pla, S., and Catalan, J.: Chrysophyte cysts from lake sediments reveal the submillennial winter/spring climate variability in the northwestern Mediterranean region throughout the Holocene. Clim. Dyn., 24, 263-278, https://doi.org/10.1007/s00382-004-0482-1, 2005.

Prahl, F. G., and Wakeham, S. G.: Calibration of unsaturation patterns in long-chain ketone compositions for palaeotemperature assessment. Nature, 330, 367, https://doi.org/10.1038/330367a0, 1987.

Prahl, F. G., Muehlhausen, L. A., and Zahnle, D. L.: Further evaluation of long-chain alkenones as indicators of paleoceanographic conditions. Geochim. Cosmochim. Ac., 52, 2303-2310, https://doi.org/10.1016/0016-7037(88)90132-9, 1998.

Ran, L., Jiang, H., Knudsen, K.L. and Eiríksson, J.: Diatom-based reconstruction of palaeoceanographic changes on the North Icelandic shelf during the last millennium. Palaeogeogr., Palaeoclimatol., Palaeoecol., 302, 109-119, https://doi.org/10.1016/j.palaeo.2010.02.001, 2011.

Richter, N., Longo, W. M., George, S., Shipunova, A., Huang, Y., and Amaral-Zettler, L.: Phylogenetic diversity in freshwater-dwelling Isochrysidales haptophytes with implications for alkenone production. Geobiology, 17, 272-280, https://doi.org/10.1111/gbi.12330, 2019.

Salacup, J. M., Farmer, J. R., Herbert, T. D., and Prell, W. L.: Alkenone Paleothermometry in Coastal Settings: Evaluating the Potential for Highly Resolved Time Series of Sea Surface Temperature. Paleoceanogr. Paleoclimatol., 34, 164-181, https://doi.org/10.1029/2018PA003416, 2019.

https://doi.org/10.5194/cp-2020-84
Preprint. Discussion started: 26 June 2020

Schmidt, G. A., Jungclaus, J. H., Ammann, C. M., Bard, E., Braconnot, P. C. T. J. D. G., Crowley, T. J., Delaygue, G., Joos, F., Krivova, N.A., Muscheler, R., and Otto-Bliesner, B. L.: Climate forcing reconstructions for use in PMIP simulations of the last millennium (v1. 0). Geosci. Model Devel., 4, 33-45, https://doi.org/10.5194/gmd-4-33-2011, 2011.

Seppä, H., Bjune, A. E., Telford, R. J., Birks, H. J. B., and Veski, S.: Last nine-thousand years of temperature variability in Northern Europe. Clim. Past, 5, 523-535, https://doi.org/10.5194/cp-5-523-2009, 2009.

Sicre, M.A., Jacob, J., Ezat, U., Rousse, S., Kissel, C., Yiou, P., Eiríksson, J., Knudsen, K.L., Jansen, E., and Turon, J.L.: Decadal variability of sea surface temperatures off North Iceland over the last 2000 years. Earth Planet. Sci. Lett., 268, 137-142, https://doi.org/10.1016/j.epsl.2008.01.011, 2008.

Sicre, M.A., Hall, I.R., Mignot, J., Khodri, M., Ezat, U., Truong, M.X., Eiríksson, J., and Knudsen, K.L.: Sea surface temperature variability in the subpolar Atlantic over the last two millennia. Paleoceanography, 26, https://doi.org/10.1029/2011PA002169, 2011.

Sigl, M., Winstrup, M., McConnell, J.R., Welten, K.C., Plunkett, G., Ludlow, F., Büntgen, U., Caffee, M., Chellman, N., Dahl-Jensen, D., and Fischer, H.: Timing and climate forcing of volcanic eruptions for the past 2,500 years. Nature, 523, 543-549, https://doi.org/10.1038/nature14565, 2015.

Steinhilber, F., Beer, J., and Fröhlich, C.: Total solar irradiance during the Holocene. Geophys. Res. Lett., 36, https://doi.org/10.1029/2009GL040142, 2009.

Sun, Q., Chu, G., Liu, G., Li, S., and Wang, X.: Calibration of alkenone unsaturation index with growth temperature for a lacustrine species, Chrysotila lamellosa (Haptophyceae). Org. Geochem., 38, 1226-1234, https://doi.org/10.1016/j.orggeochem.2007.04.007, 2007.

Theroux, S., D'Andrea, W. J., Toney, J., Amaral-Zettler, L., and Huang, Y.: Phylogenetic diversity and evolutionary relatedness of alkenone-producing haptophyte algae in lakes: implications for continental paleotemperature Earth Planet. Sci. Lett., 300, 311-320, https://doi.org/10.1016/j.epsl.2010.10.009, 2010.

Theroux, S., Toney, J., Amaral-Zettler, L., and Huang, Y.: Production and temperature sensitivity of long chain alkenones in the cultured haptophyte Pseudoisochrysis paradoxa. Org. Geochem., 62, 68-73, https://doi.org/10.1016/j.orggeochem.2013.07.006, 2013.

Toohey, M., and Sigl, M.: Volcanic stratospheric sulphur injections and aerosol optical depth from 500 BCE to 1900 CE. Earth Syst. Sci. Data, 9, 809-831, https://doi.org/10.5194/essd-9-809-2017, 2017.

Toney, J. L., Huang, Y., Fritz, S. C., Baker, P. A., Grimm, E., and Nyren, P.: Climatic and environmental controls on the occurrence and distributions of long chain alkenones in lakes of the interior United States. Geochim. Cosmochim. Ac., 74, 1563-1578, https://doi.org/10.1016/j.gca.2009.11.021, 2010.

Toney, J. L., Theroux, S., Andersen, R. A., Coleman, A., Amaral-Zettler, L., and Huang, Y.: Culturing of the first 37: 4 predominant lacustrine haptophyte: geochemical, biochemical, and genetic implications. Geochim. Cosmochim. Ac., 78, 51-64, https://doi.org/10.1016/j.gca.2011.11.024, 2012.

https://doi.org/10.5194/cp-2020-84
Preprint. Discussion started: 26 June 2020

van der Bilt, W. G., D'Andrea, W. J., Bakke, J., Balascio, N. L., Werner, J. P., Gjerde, M., and Bradley, R. S.: Alkenone-based reconstructions reveal four-phase Holocene temperature evolution for High Arctic Svalbard. Quat. Sci. Rev., 183, 204-213, https://doi.org/10.1016/j.quascirev.2016.10.006, 2018.

Van Nieuwenhove, N., Pearce, C., Knudsen, M. F., Røy, H., and Seidenkrantz, M. S.: Meltwater and seasonality influence on subpolar Gyre circulation during the Holocene. Palaeogeogr., Palaeoclimatol., Palaeoecol., 502, 104-118, https://doi.org/10.1016/j.palaeo.2018.05.002, 2018.

Wang, Z., and Liu, W.: Calibration of the $U_{37}^{K'}$ index of long-chain alkenones with the in-situ water temperature in Lake Qinghai in the Tibetan Plateau. Chinese Sci. Bull., 58, 803-808, https://doi.org/10.1007/s11434-012-5527-y, 2013.

Wang, J., Yang, B., Ljungqvist, F. C., Luterbacher, J., Osborn, T. J., Briffa, K. R., and Zorita, E.: Internal and external forcing of multidecadal Atlantic climate variability over the past 1,200 years. Nature Geosci., 10, 512-517, https://doi.org/10.1038/ngeo2962, 2017.

Yeager, S. G., and Robson, J. I.: Recent progress in understanding and predicting Atlantic decadal climate variability. Curr. Clim. Change Rep., 3, 112-127, https://doi.org/10.1007/s40641-017-0064-z, 2017.

Yoshimori, M., Stocker, T. F., Raible, C. C., and Renold, M.: Externally forced and internal variability in ensemble climate simulations of the Maunder Minimum. J. Clim., 18, 4253-4270, https://doi.org/10.1175/JCLI3537.1, 2005.

Zanchettin, D., Timmreck, C., Graf, H.F., Rubino, A., Lorenz, S., Lohmann, K., Krüger, K. and Jungclaus, J.H.: Bi-decadal variability excited in the coupled ocean–atmosphere system by strong tropical volcanic eruptions. Clim. Dyn., 39, 419-444, https://doi.org/10.1007/s00382-011-1167-1, 2012.

Zheng, Y., Huang, Y., Andersen, R. A., and Amaral-Zettler, L. A.: Excluding the di-unsaturated alkenone in the U_{37}^{K} index strengthens temperature correlation for the common lacustrine and brackish-water haptophytes. Geochim. Cosmochim. Ac., 175, 36-46, https://doi.org/10.1016/j.gca.2015.11.024, 2016.

Zink, K. G., Leythaeuser, D., Melkonian, M., and Schwark, L.: Temperature dependency of long-chain alkenone distributions in recent to fossil limnic sediments and in lake waters. Geochim. Cosmochim. Ac., 65, 253-265, https://doi.org/10.1016/S0016-7037(00)00509-3, 2001.